Haptic-Enhanced Virtual Reality Simulator for Robot-Assisted Femur Fracture Surgery*

Fayez H. Alruwaili, David W. Halim-Banoub, Jessica Rodgers, Adam Dalkilic, Christopher Haydel, Javad Parvizi, Iulian I. Iordachita, Mohammad H. Abedin-Nasab

Abstract — In this paper, we develop a haptic-enhanced virtual reality (VR) simulator for the Robossis robot-assisted femur fracture surgery. Given the complex nature of robotassisted surgery and its steep learning curve, a dedicated training tool is vital for equipping surgeons with the necessary skills to effectively operate the surgical system. We develop the Robossis Surgical Simulator (RSS) to closely replicate the surgical environment of the Robossis system. The user interacts with the RSS using external hardware that includes the Sigma-7 Haptic Controller and the Meta Quest VR headset. Further, we implement the separating axis theorem to retrieve the collision between the distal and proximal bone segment and, hence, determine the required haptic feedback that restricts the bonebone collision. This development demonstrates a promising avenue and a novel approach to enhance the training protocol for the Robossis system.

I. INTRODUCTION

Surgical competence is achieved through hours of practice and failure using models under the supervision of a limited number of highly specialized surgeons [1]. This can be very time-consuming and costly for future specialized surgeons to attain the experience needed for operational proficiency. Virtual reality (VR) simulators allow residents and skilled surgeons to learn new complex surgical procedures through failure with low risk [2]. Through VR training, surgeons have demonstrated shortened surgical times, greater tool dexterity, and greater accuracy in the operating room [3]. Furthermore, VR simulators equipped with haptic feedback have demonstrated improved skill acquisition and added a crucial layer of realism and interactivity. This enhancement is evident in various applications, including but not limited to laparoscopy and dental training [4], [5].

Currently, femur fracture surgery has a high risk of

*This work is funded by the National Science Foundation (NSF) under grants 2141099, and 2226489, and by the New Jersey Health Foundation (NJHF) under grant PC 62-21.

- F. A, A. D, and M. A are with the Biomedical Engineering Department, Rowan University, Glassboro, NJ 08028, USA (e-mail: alruwa16@rowan.edu, dalkil38@students.rowan.edu corresponding author's email: abedin@rowan.edu).
- D. H is with Rowan-Virtua School of Osteopathic Medicine, Stratford, NJ 08084, USA(e-mail: halimb73@rowan.edu)
- J. R is with the Mechanical Engineering, Rowan University, Glassboro, NJ 08028, USA (e-mail: rodger58@students.rowan.edu).
- C. Haydel is an Orthopedic Trauma Surgery with Virtua Health, Moorestown, NJ 08057 (e-mail: chaydel@virtua.org)
- J. Parvizi is with Rothman Orthopedic Institute, Thomas Jefferson University Hospital, Philadelphia, Pennsylvania (e-mail: javadparvizi@gmail.com).
- I. I. is with the Laboratory for Computational Sensing and Robotics, Johns Hopkins University, Baltimore, MD 21218 USA (e-mail: iordachita@jhu.edu).

surgical complications, including high malalignment rates and high fracture reduction forces [6], [7]. In the past, our group presented a surgical system called Robossis that aids in eliminating the challenges during femur fracture surgery [8]-[10]. Robossis has shown the potential to eliminate these complications through cadaveric and benchtop studies, but user training is required to maximize fluidity and success rate

II. RELATED WORK AND CONTRIBUTION

The number of robot-assisted surgeries continues to grow annually, and the training of surgeon(s) and operating staff to utilize these devices effectively has been investigated. In the past, a variety of surgical simulators, including RoSS, dV-Trainer, dVSS, and SEP, were developed to provide surgeon(s) with the required skills to operate the varying surgical robotic systems [11]-[13]. Multiple studies validated the effectiveness of the training regime using the surgical simulators, which shows a significant improvement in surgical proficiency translated to the operating room [11]-[13].

Motivated by these remarks, we aim to develop the Robossis Surgical Simulator (RSS) that is designed specifically for the implementation of the Robossis system during femur fracture surgeries. We aim to provide the surgeon(s) and operating staff with the required training resources for the Robossis system. The RSS is developed to immerse the users in a 3D environment utilizing the Meta Quest VR headset (Meta – United States) and haptic feedback via the Sigma.7 haptic controller (Force Dimension – Switzerland). Furthermore, we leverage Unreal Engine with high-end graphics and advanced rendering capabilities for creating a high-quality VR environment. The key aspects of our design and development in this paper are the following:

- 1. We design and develop the RSS that inherits a surgical environment as previously completed in a cadaver experiment. Also, we design a control architecture that integrates the user to the VR environment using the HC and Meta Quest VR headset. Further, we leverage the tools of unreal engines to provide 2D fluoroscopic imaging and user interface (UI) widgets within the VR environment.
- 2. We develop the kinematic representation of the Robossis Surgical Robot (RSR) and Sigma.7 Haptic Controller (HC) within the surgical simulator. We implement a motion controller to drive the joints of the RSR and HC as resembled in the real world. We validate the kinematic representation by performing simulation error analysis.

3. We develop a haptic feedback collision algorithm that projects forces onto the user's hand via the HC to prevent an overlap between the proximal and distal bone segments. We model the proximal and distal bones as an oriented bounding box (OBB) and retrieve the collision utilizing the separating axis theorem. Thus, 4 OBBs are designed to cover the shaft, distal, and proximal segments of the femur bone for realistic real-life modeling. Further, we regulate the axis control for the RSR using haptic feedback. Each axis (translation and rotation) is modeled as a spring-damping system to provide the required haptic feedback that restricts the motion in each specified locked axis.

III. ARCHITECTURE OF THE ROBOSSIS SURGICAL SIMULATOR

The architecture of the RSS is illustrated in Fig. 1. The VR environment was designed using Unreal Engine 5.2.1 and Blender 3.6. We use the HC as the interface between the user input trajectories (X_{HC}) and speed (\dot{X}_{HC}) into the VR environment to the manipulation of the RSR. We implement a motion control algorithm that scales user input trajectories to a maximum linear and angular velocity to represent conditions similar to those in the real world. Also, we develop the kinematic representation of the RSR and HC to resemble real-world physical structures. We interface the inverse kinematics of the RSR and HC to drive the joints of the RSR $(d_{RSR,i}, \theta_{RSR,i})$ and HC $(\theta_{HC,i})$ and manipulate the end-effector of each robot to the desired location and orientation within the RSS. Also, we implement haptic feedback algorithms that restrict the overlap between the distal (D) and proximal (P) bone segments $(D \cap P)$, and regulate the motion for each axis (F_{lock}, τ_{lock}) . Additionally, we incorporate the Meta Quest VR headset to immerse the user into a 3D virtual environment by using the Oculus VR plugin impeded within the unreal engine. Also, we utilize the input from the Oculus headset to provide the user with additional control over the orientation of the c-arm to capture the 2D fluoroscopic imaging and regulate each axis.

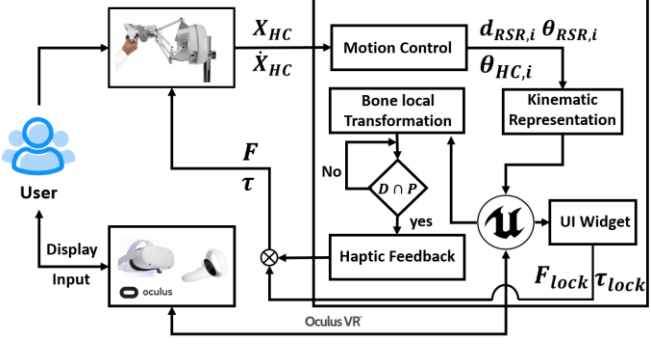


Figure 1. The architecture of the designed RSS is illustrated, where the entire architecture includes the haptic Sigma-7 controller, the Metal Quest VR headset, control algorithms, kinematic representation, haptic feedback, and the Unreal Engine simulator to house the VR environment.

IV. SIMULATOR DESIGN AND MODELING

The RSS was modeled to resemble an actual operating room for the Robossis system surgical setting for femur fracture surgery, as previously completed in a cadaver experiment (Fig. 2)[10].

A. Surgical Environment Design

The RSS was designed using Unreal Engine 5.2.1 and Blender 3.6. The RSS includes the HC, a surgeon workstation, RSR, the patient placed in the supine position, and the C-arm X-ray machine. Also, the RSR is attached to the patient's distal femur using surgical rods. Blender software was used to provide the required enhancement for the visual rendering of the meshes. For example, Blender was used to add draping on the patient, color meshes, and establish the reference frame for the translation and orientation of the meshes. Furthermore, the RSS, inherited from a VR template, was designed to interface the environment with external hardware control algorithms and house the surgical simulator. Additionally, the simulation was designed for integration with the Meta Quest headset to establish an immersive and in-depth VR environment. The Meta Quest controller was integrated to facilitate secondary simulation controls. This controller takes user input to direct the C-Arm X-ray position and rotation, enabling various anatomical planar views of the surgical field, which are consistently updated, producing a real-time display X-ray imaging monitor.



Figure 2. A previous cadaver experiment using the Robossis System. The surgical setting includes (1) a haptic controller, (2) a surgeon workstation, (3) the Robossis Surgical robot, (4) a cadaver patient, and (5) a C-arm X-ray machine.

B. Robot Kinematic Representation

Robossis system consists of a leader, HC Sigma.7, and a follower, RSR. The Sigma.7 HC is a hybrid robot structure based on a delta mechanism providing 3-DOF translational manipulation, a wrist serial mechanism providing 3-DOF rotational manipulation, and a grasping unit for 1-DOF (Fig. 3A). To define the kinematic representation of the HC in the unreal engine, the HC components were divided into varying links (L_{HC}1-9) and connected via joints (J_{HC} A_i-H_i) using the parent-child convention to define the relationship between the links (Fig. 3A). For each of the ith arm of the delta mechanism, it consists of one active joint (J_{HC} A_i) and six passive joints (J_{HC} C_i-E_i). Further, each arm is connected to a

fixed base (L_{HC} 6) connected to the serial wrist mechanism. The wrist serial mechanism consists of three active joints (J_{HC} F-H) responsible for the three independent axes of rotation ($\alpha \beta \gamma$).

Additionally, the follower RSR is a 3-armed parallel mechanism where each ith arm is placed on a moving and fixed ring (Fig. 3B). The RSR is designed to meet the clinical and mechanical requirements for femur fracture surgery, including 1) applying traction forces/torques, 2) precise alignment, and 3) holding bone fragments for fixation. To represent RSR in the unreal engine, the robot components are divided into varying links (LRSR1-5) and connected via joints (JRSR Ai-Di) using the parent-child convention to define the relationship between the links (Fig. 3B). Each arm of the Robossis surgical robot includes three joints: universal (represented as an active and passive joint (Jrsr Ai & Jrsr B_i), prismatic (J_{RSR} C_i), and spherical (J_{RSR} D_i) (Fig. 3B). The universal joint (LRSR 2i) connects the rotary actuator shaft (L_{RSR}1) to the lower arm (L_{RSR} 3_i) and is placed in the fixed platform. Also, the spherical joint connects the upper parts of the linear actuators (LRSR 4i) to the moving ring $(L_{RSR} 5_i).$

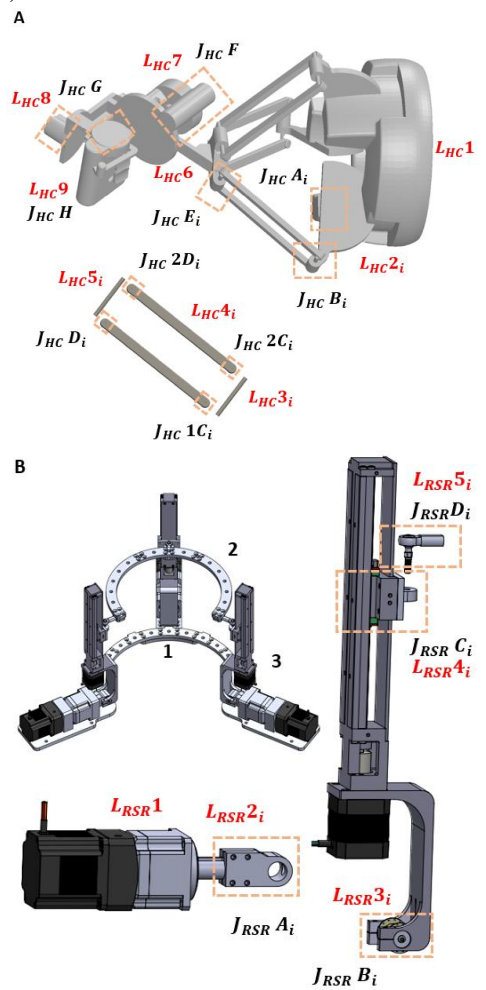


Figure 3. Kinematic representation of the leader-follower Robossis system within unreal engine. A & B) The HC Sigma. 7 and RSR strucutre is divided into vary links and connected via joints to define a closed-loop link-joint relationship that resemble the actual real-world. B) RSR structure include a fixed ring (1), a moving ring (2), and three arms (3) where each arm consists of a linear and rotary actuator.

C. 2D Fluoroscopic Imaging

We developed 2D fluoroscopic imaging within the RSS to enable various anatomical planar views of the surgical field. The 2D fluoroscopic imaging was developed by utilizing the scene capture 2D tool within the unreal engine. The scene capture 2D setting is specified to show only components within the surgical setting, including the patient's thigh, proximal and distal bone, and the RSR. Furthermore, the material properties of the patient thigh and bone were optimized to create an x-ray-like effect. Specifically, the material properties were set to an additive blended mode with opacities for the bone and thigh materials of 0.8 and 0.1, respectively. Also, the scene capture 2D was set as a child of the C-arm static mesh to receive input from the Meta Quest controller for the user-desired global rotation.

V. HAPTIC CONTROLLER AND MOTION CONTROL

A. Motion Control

We drive the motion of the leader Sigma.7 HC active joints ($\theta_{HC,i}$, labeled in Fig3. A as $J_{HC}A_{1-3}$, $J_{HC}F$, $J_{HC}G$, and $J_{HC}H$) and the follower RSR active joints ($\theta_{RSR,i}$, labeled in Fig3. B as $J_{RSR}A_i$) and linear actuators ($d_{RSR,i}$, labeled in Fig3. B as $J_{RSR}C_{1-3}$) within Unreal Engine to recreate realistic real-world movement. As described earlier, the Sigma.7 HC is a hybrid structure composed of a delta mechanism with three active joints ($\theta_{HC,1-3}$) and a wrist mechanism with three active joints ($\theta_{HC,1-6}$). We determine the active joint angles ($\theta_{HC,1-6}$) from the HC (Force Dimension SDK) library. As such, we interface the active joint values into the RSS-designed blueprint to drive the HC end-effector into the theoretical global position and orientation.

Furthermore, the HC Sigma-7 end-effector global position and orientation trajectories, as commanded by the user's hand, are interfaced with the RSR as an incremental trajectory as

where $x(t)_{RSR} = x_{RSR}(t-1) + S * (x(t)_{HC} - x(t-1)_{HC})$ (1) where $x(t)_{RSR} \in R^6$ and $x_{RSR}(t-1) \in R^6$ are the current and previous location of the RSR, and $x(t)_{HC} \in R^6$ and $x(t-1)_{HC} \in R^6$ are the current and previous location of the HC (user's hands). Also, $S \in R^{6x6}$ is the dynamic scaling factor, and it is defined as

where
$$\|\boldsymbol{v}_{HC}\|$$
 and $\|\boldsymbol{\omega}_{HC}\|$ are the norms of the linear and

where $\|v_{HC}\|$ and $\|\omega_{HC}\|$ are the norms of the linear and angular velocities of the HC (user's hands) during motion $\sim \dot{x}(t)_{HC} \in \mathbb{R}^6$. Also, Max_v , Max_ω are the desired maximum linear and angular velocities based on the user's desired input, and I_{nxn} is identity matrix with n rows and n columns.

Further, we map the input of the user's hand-scaled trajectory's location and orientation $(x(t)_{RSR})$ as the desired location of the Robossis end effector (center of the moving ring (P)). Given the position (P(x, y, z)) and orientation $(R(\alpha, \beta, \gamma))$ of the endpoint effector (P), the length of the linear actuator $(d_{RSR,i})$ and the rotation of the active joint $(\theta_{RSR,i})$ are computed as derived in our previous work [8]—

[10]

Given the desired position of the linear actuator $(d_{RSR,i})$ as well as the active joints angles of the RSR $(\theta_{RSR,i})$ and HC $(\theta_{HC,i})$, we specify the angular drive parameter for each joint within Unreal Engine to define the physical strength of the joints (stiffness, damping, and maximum force limit). Algorithm 1 below describes the overall procedure used to drive the HC, and RSR in the RSS simulator. The algorithm is a blueprint C++ inherited class designed for the RSS to interface the HC and control the motion of the RSR and HC.

Algorithm 1: Motion Control

```
1: MotionControl::BeginPlay () {
2: ActiveJoint i->SetAngularDriveParams(stiffness, damping, force)
    ActiveJoint_i->SetAngularOrientationDrive(true, true)
    LinearJoint i->SetLinearDriveParams(stiffness, damping, force)
5: LinearJoint i->SetLinearPositionDrive(true,true,true)
7: MotionControl::Tick(DeltaTime) {
8: [x(t)_{HC}] = \text{Sigma}_7 \rightarrow \text{GetPositionRotation}()
    [\dot{x}(t)_{HC}] = \text{Sigma}_{7} \rightarrow \text{GetLinearAngularSpeed} ()
10: [\|v_{HC}\|, \|\omega_{HC}\|] \rightarrow \operatorname{norm}(\dot{x}(t)_{HC})
11: If (\|\boldsymbol{v}_{HC}\|, \|\boldsymbol{\omega}_{HC}\| > Max_v, Max_\omega)
12:
            S \rightarrow Eq.(2)
13: Else
            S = I_{6x6};
14:
15.
16: x(t)_{RSR} \rightarrow Eq.(1)
17: Robossis_Kinematics(x(t)_{RSR})
18: SetLinearPositionTarget(d_{RSR,t})
19: SetAngularOrientationTarget(\theta_{RSR,i})
20: [\theta_{HC,t}] = Sigma_7 \rightarrow GetJointAngles()
21: SetAngularOrientationTarget(\theta_{HC,t})
```

B. Haptic Feedback: Bone Collision

We develop a haptic feedback bone collision algorithm to prevent the user from overlapping the distal (D) and proximal (P) bone $(D \cap P)$. We model the proximal bone as a fixed oriented bounding box (OBB) while the distal bone is modeled as a moving OBB with respect to the center of the moving ring of the RSR (Fig. 4). 4 OBBs are designed to cover the shaft, distal, and proximal segments of the femur bone for realistic modeling.



Figure 4. Oriented bounding boxes (OBB) for the proximal bone (A) and distal bone (B) model is illustrated. A total of 4 OBBs are designed to cover the shaft, distal, and proximal segments of the femur bone for a realistic modeling.

We implement the separating axis theorem (SAT) [14] to detect the collision between the proximal and distal bone OBBs. As such, we develop the collision algorithm to check if there is an overlap between the proximal and distal OBBs for each potential separating axis (\boldsymbol{L}) that includes the 3-faces normal for each of the OBBs and the additional 9 potential separating axes arising from the cross products between the edges of OBBs. Therefore, there are 15 possible separating

axes that we need to verify to determine if there is a collision occurring between 2 OBBs, one from the proximal end and one from the distal end. Since the proposed model consists of 2 proximal OBBs and two distal OBBs, we check if there is a collision between each distal OBB with respect to the proximal OBB.

Algorithm 2: Haptic feedback bone collision

```
1: For (1 to 2) { \\ Each distal OOB
     For (1 to 2) { \\ Each proximal OBB
       C_{OBB,P}, C_{OBB,D} \rightarrow proximal and distal center local (XYZ) position
        A_{x,\text{OBB,P}}, A_{y,\text{OBB,P}}, A_{z,\text{OBB,P}} \rightarrow \text{local faces axis of OBB P}(R_P^{3X3})
        A_{x,OBB,D}, A_{y,OBB,D}, A_{z,OBB,D} \rightarrow \text{local faces axis of OBB D } (R_n^{3\chi3})
5:
        SmallestOverlap → inf
6.
        // Check OBBs faces and edges
        AXIS = [R_P^{3X3}, R_D^{3X3}, cross(R_P^{3X3}(i,:), R_D^{3X3}(j,:))] // i \& j (1 to 3)
        For (i = 1 to 15) // for each potential separating axis
9:
10:
            L = AXIS(:,i)
            E_{OBB,P}, E_{OBB,D} \rightarrow \text{Eq. } 3
11:
12:
            BE_{OBB,P}, BE_{OBB,D} \rightarrow \text{Eq. 4}
            OL \rightarrow Eq. 5
13:
            If (OL < 0) // a separating axis
14:
               d = 0
15:
16:
               \hat{n} = [0 \ 0 \ 0]
17.
               return
18:
            Else // a collision detected
               If (OL < SmallestOverlap)
20:
                    SmallestOverlap → d
21:
                    If ((\boldsymbol{C}_{OBB,D} - \boldsymbol{C}_{OBB,P}) \cdot \boldsymbol{L} > \boldsymbol{0}) \setminus \text{direction of the norm}
22:
                        \widehat{n} \rightarrow L
23.
                    Else
                         \widehat{n} \rightarrow -L
25:
      F_{col} += Eq. 6 (sum forces)
26: F_{tot} \rightarrow \text{Eq. } 7
27: Sigma_7 \rightarrow SetForce([F_{tot}(x, y, z)]
```

Given each potential separating axis (L), the projection of the OBBs extent into the potential separating axes is estimated as:

 $E = W_x |proj_L A_x| + W_y |proj_L A_y| + W_z |proj_L A_z|$ (3) where W_x , W_y , and W_z are the half length of the OBBs faces, L is the potential separating axes, and A_x , A_y , and A_z are the axis of each of the local faces of the OBBs. Each column vector A_x , A_y , and A_z corresponds to the R rotation matrix following Euler angles (X-Y-Z). Furthermore, the maximum and minimum extent of the OBBs that is projected into the potential separating axes (L) can be estimated as:

$$BE = proj_L C \pm E \tag{4}$$

Where C is the local XYZ center of the OBBs. As such, we can determine if there is an overlap (OL) between a distal and proximal OBBs as:

$$OL = min(maxBE_{OBB,P}, maxBE_{OBB,D}) - max(minBE_{OBB,P}, minBE_{OBB,D})$$
(5)

Where OL is the overlap between the maximum and minimum extent of the OBBs from each distal and proximal segment. Given the iteration along the potential separating axis, OL < 0 indicates the presence of a separating axis; therefore, a collision is not present. On the other hand, if OL > 0 for each potential separating axis (L), a collision is present. As such, the force restriction that prevents the overlapping between the proximal and distal bone segments is modeled as:

$$\boldsymbol{F_{Col}} = k_c * d * \widehat{\boldsymbol{n}} \tag{6}$$

where F_{col} is the force vector at the contact of the collision, d is the penetration depth, \hat{n} is the norm of the force, and k_c is

the spring constant (1000 N/m). OL with the smallest overlap corresponds to the penetration depth (d) with a normal vector corresponding to the face of the collision (\hat{n}) . Further, the direction of the norm $(\hat{\mathbf{n}})$ is based on the alignment of the vector originating from the center of the colliding distal OBB to the proximal OBB projected on the potential separating axis (L). Thus, F_{tot} is the sum due to the collision of each distal OBB with respect to the proximal OBB. Hence, the global force is estimated as:

$$F_{tot} = F_{Col} - \mathbf{c} \cdot \mathbf{v} \tag{7}$$

 $F_{tot} = F_{Col} - c \cdot v$ (7) where v is velocity vector and c is the damping constant (10) N s/m). An illustration of the haptic feedback bone collision method is presented in algorithm 2.

C. UI Widget Axis Control

N/m and 0.1 Nm/deg).

We designed an interactive user interface (UI) widget to provide the user with axis control of the RSR. The UI widget is designed as a blueprint that receives inputs from the user via the Meta Quest controller and casts the signals that regulate the haptic feedback applied onto the user's hand. Each axis (translation and rotation) is modeled as a springdamping system to provide the required haptic feedback to restrict the motion of the user in each specified locked axis

$$F_{lock} = -k_f * (\mathbf{x}(\mathbf{t})_{HC,xyz} - \mathbf{x}_{lock,xyz}) - c_f * \mathbf{v}_{HC}$$
 (8)
 $\mathbf{\tau}_{lock} = -k_{\tau} * (\mathbf{x}(\mathbf{t})_{HC,\alpha\beta\gamma} - \mathbf{x}_{lock,\alpha\beta\gamma}) - c_{\tau} * \boldsymbol{\omega}_{HC}$ (9)
where $F_{wall} \in R^3$ and $\mathbf{\tau}_{wall} \in R^3$ are the force and torque vectors applied at the specified locked axis, respectively. Also, c_f and c_{τ} are the damping constant (10 N s/m and 0.001 Nm s/deg); and k_f and k_{τ} are the spring constant (1000

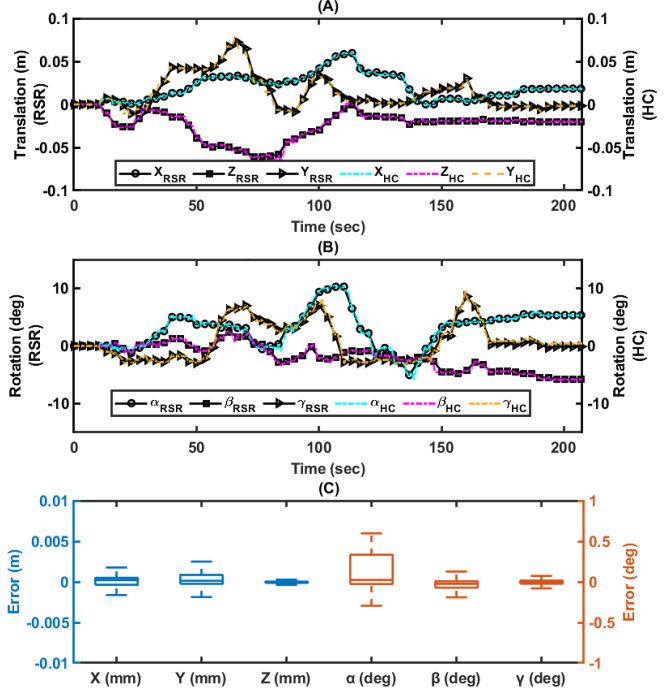


Figure 5. (A & B) RSR trajectory as commanded by the user's hand via the HC Sigma-7. (C) The corresponding error analysis is performed to determine the deviation of the RSR from the HC.

VI. SIMULATION AND TESTING

A. Robossis Kinematic Interface

The deviation of the RSR from the motion of the user's hand via the Sigma-7 HC was evaluated. As the simulation proceeded, the user simultaneously manipulated the RSR in all 6-DOF (translational and rotational). Fig. 5A & B present the corresponding trajectories from the RSR (left) and HC (right). We performed an error analysis to determine the deviation of the RSR from the HC (Fig. 5C). Fig. 5C illustrates a maximum variation for translation and rotation as ~ 5 mm and ~ 0.6 deg, respectively.

B. Haptic Feedback

The haptic feedback bone collision algorithm is implemented to recreate a realistic scenario to the real physical world. The modeling of OBBs was required due to the curved structure of the femur bone and the 6-DOF movement of the distal bone with respect to the center of the moving ring of the RSR. The simulation analysis illustrated in Fig. 6 presents a 2D fluoroscope imaging and the haptic feedback projected by the haptic controller into the user during the simulation. Fig. 6 A-F shows varying collision scenarios of the bone segments where, in each presented scenario, the force vector restricts the user's attempts to further penetrate the colliding surface of the bone

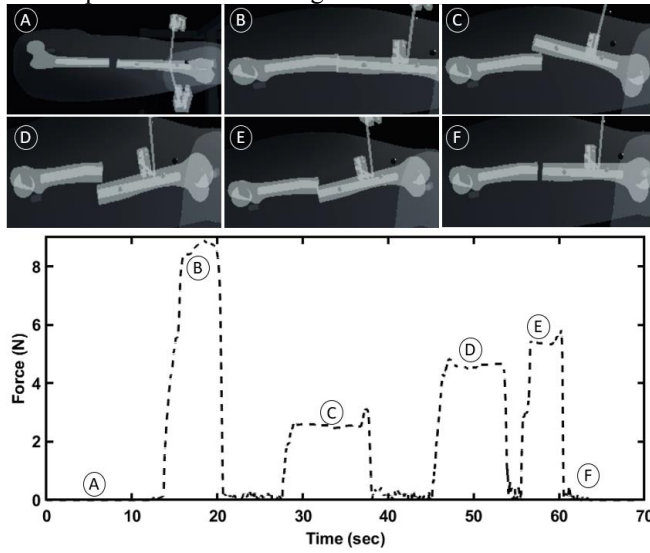


Figure 6. Haptic feedback of the bone collision algorithm between the proximal and distal bone segments is illustrated. We present 2D fluoroscope imaging above the haptic feedback applied by the haptic controller onto the user during the simulation. A-F shows varying collision scenarios of the bone segments where the force vector restricts the user attempts to further penetrate to the colliding surface of the bone on each scenario.

C. Integrated Simulation Environment

The RSS environment was created to immerse the trained users in a realistic operating room environment for femur fracture surgery using the Robossis system (Fig. 7). To interact with the environment, the HC Sigma-7 was used to manipulate the distal bone segment in the desired translational and rotational directions (attached video). As the user manipulates the HC, real-time visual rendering for the location of the bone is displayed as 2D fluoroscopic imaging via the Meta Quest headset. Utilizing the Meta Quest controller, the user is able to rotate the c-arm to the desired anatomical planar views and regulate the axis of the RSR. Also, with the implementation of the HC, the user is prevented from overlapping the moving distal bone (attached to the RSR) with the proximal bone to recreate a realistic condition.

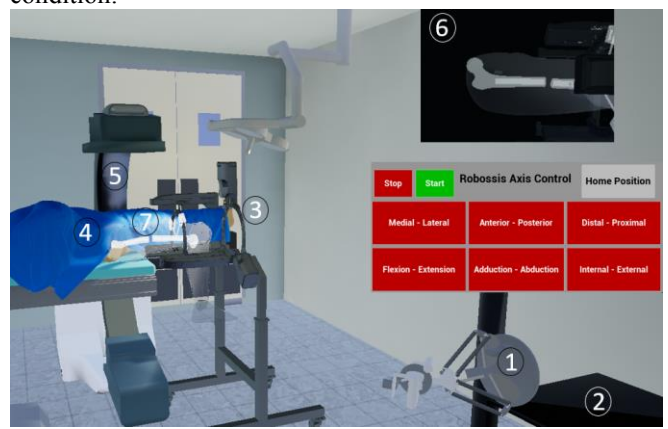


Figure 7. Robossis-assisted femur fracture surgery environment was designed to include (1) a haptic controller, (2) a surgeon workstation, (3) the Robossis surgical robot, (4) a cadaver patient, (5) a C-arm X-ray machine, and (6) real-time visual rendering of the location of the bone is displayed as 2D fluoroscopic imaging. The Robossis surgical robot is attached to the distal bone segment using surgical rods (7). The environment was created with the goal to immerse the trained users in a similar operating room environment for femur fracture surgery using the Robossis system.

VII. DISCUSSION

The RSS is designed with the goal of immersing the user in a realistic environment, as previously completed in a cadaveric study. Therefore, surgeons and operating staff will better translate their techniques to the real world. This replication allows the surgeons to gain a more spatial and visual feel that eliminates adjustments needed for the real-world transition. Also, the RSS is designed to provide future trainees with the necessary tools to enhance surgical efficacy for the integration of the RSR in the clinical field.

Further, the proposed methods for the development of the RSS present a novel approach for the representation of digital robots and integration with real-world systems. Specifically, the kinematic representation and matching between the real-world HC Sigma-7, RSR, and the virtual RSR and HC yields real-time evaluation during surgical training. This kinematic matching ensures that the RSR follows the desired motion as the surgeon manipulates the HC. Additionally, the integration of haptic feedback into the RSS provides users with the virtual representation and collision of the bone segments during the training. Thus, realistic behavior is experienced during training on the simulator.

For future work, we plan to determine the RSS's usability with surgeons and operating staff to get feedback on the experience-based learning for the Robossis system. We will determine the RSR's usability by evaluating the user's ability to align different cases for femur fractures (distal, shaft, and proximal) within the RSS. We will determine the user success rate and time for completion. Lastly, we will use the NASA Task Load Index to assess the workload with trials.

VIII. CONCLUSION

In this study, we were able to develop a haptic-enhanced VR simulator specifically designed for the Robossis system femur fracture procedure. This development provides a realistic replication of the Robossis surgical setting, enabling future trainees to comfortably and confidently gain experience in a low-risk, cost-effective environment. The incorporation of VR, and haptic feedback added a vital layer of realism and interactivity, which is anticipated to significantly improve skill acquisition for future trainees. Further, this innovative training regime is expected to facilitate a more engaging and immersive learning experience, bridging the gap between theoretical knowledge and practical skills. This advancement in training not only enhances the learning curve but also promises to elevate the standard of medical education and patient care.

REFERENCES

- M. P. Rogers, A. J. DeSantis, H. Janjua, T. M. Barry, and P. C. Kuo, "The future surgical training paradigm: Virtual reality and machine learning in surgical education," *Surgery*, vol. 169, no. 5, pp. 1250– 1252, 2021.
- [2] A. J. Lungu, W. Swinkels, L. Claesen, P. Tu, J. Egger, and X. Chen, "A review on the applications of virtual reality, augmented reality and mixed reality in surgical simulation: an extension to different kinds of surgery," *Expert Rev Med Devices*, vol. 18, no. 1, pp. 47–62, 2021.
- [3] M. P. Fried et al., "From virtual reality to the operating room: the endoscopic sinus surgery simulator experiment," Otolaryngology— Head and Neck Surgery, vol. 142, no. 2, pp. 202–207, 2010.
- [4] C. Våpenstad, E. F. Hofstad, T. Langø, R. Mårvik, and M. K. Chmarra, "Perceiving haptic feedback in virtual reality simulators," *Surg Endosc*, vol. 27, pp. 2391–2397, 2013.
- [5] S. Patil et al., "Effectiveness of haptic feedback devices in preclinical training of dental students—a systematic review," BMC Oral Health, vol. 23, no. 1, p. 739, 2023.
- [6] R. L. Jaarsma, Rotational malalignment after fractures of the femur. [Sl: sn], 2004.
- [7] T. Gösling et al., "Forces and torques during fracture reduction: Intraoperative measurements in the femur," *Journal of orthopaedic research*, vol. 24, no. 3, pp. 333–338, 2006.
- [8] F. Alruwaili, M. S. Saeedi-Hosseiny, L. Guzman, S. McMillan, I. I. Iordachita, and M. H. Abedin-Nasab, "A 3-Armed 6-DOF Parallel Robot for Femur Fracture Reduction: Trajectory and Force Testing," in 2022 International Symposium on Medical Robotics (ISMR), IEEE, 2022, pp. 1–6.
- [9] M. S. Saeedi-Hosseiny, F. Alruwaili, S. McMillan, I. Iordachita, and M. H. Abedin-Nasab, "A Surgical Robotic System for Long-Bone Fracture Alignment: Prototyping and Cadaver Study," *IEEE Trans Med Robot Bionics*, pp. 1–1, 2021, doi: 10.1109/TMRB.2021.3129277. Available: https://ieeexplore.ieee.org/document/9621225/
- [10] M. S. Saeedi-Hosseiny et al., "Automatic Alignment of Fractured Femur: Integration of Robot and Optical Tracking System," IEEE Robot Autom Lett, 2023.
- [11] A. J. Hung *et al.*, "Concurrent and predictive validation of a novel robotic surgery simulator: a prospective, randomized study," *J Urol*, vol. 187, no. 2, pp. 630–637, 2012.
- [12] D. J. Kiely et al., "Virtual reality robotic surgery simulation curriculum to teach robotic suturing: a randomized controlled trial," J Robot Surg, vol. 9, pp. 179–186, 2015.
- [13] S. F. Hardon, A. Kooijmans, R. Horeman, M. van der Elst, A. L. A. Bloemendaal, and T. Horeman, "Validation of the portable virtual reality training system for robotic surgery (PoLaRS): a randomized controlled trial," Surg Endosc, vol. 36, no. 7, pp. 5282–5292, 2022.
- [14] Dae Hyun Kim, Nak Yong Ko, Geum Kun Oh, and Yong Dong Kim, "A framework for haptic rendering system using 6-DOF force-feedback device," Proc IEEE Int Conf Robot Autom, vol. 1, pp. 874–879, 2001, doi: 10.1109/robot.2001.932660.